TMAP modeling of D release from baked multi-layer Be–D co-deposits

M J Simmonds[1,3] , **M J Baldwin**[1] , **G De Temmerman**[2] and **R P Doerner**[1]

[1] Center for Energy Research, UC San Diego, 9500 Gilman Dr., La Jolla, CA 92093-0417, United States of America
[2] ITER Organization, Route de Vinon-sur-Verdon, F-13067, St.-Paul-lez-Durance Cedex, France

E-mail: msimmonds@eng.ucsd.edu

CrossMark

Abstract

Single-layer Beryllium–Deuterium (Be–D) co-deposits were analyzed using Thermal Desorption mass Spectrometry (TDS) as outlined in the companion paper (Baldwin *et al* 2019 *Phys. Scr. PFMC Proc.*). This work details the TMAP modeling and the analysis of selected samples that received double-layer (DL) coatings to study co-deposit thickness and prior bake effects. TDS data were simulated with detrap energies 0.8, 0.9, and 1.0 eV. In DLs formed at 393 K, modeling revealed that under-layers baked at 623 K for either 2 or 20 h had little pumping effect on over-layers, suggesting empty trap removal during bake. Extrapolated to ITER, data and analysis suggest less impact on the ongoing ITER bake efficiency than previously predicted (Baldwin and Doerner 2015 *J. Nucl. Mater.* **467** 38391).

(Some figures may appear in colour only in the online journal)

1. Introduction

Tritium (T) retention in ITER PFMs will be dominated by Be-HI (Hydrogen Isotope) co-deposition [1]. The Be-clad first wall will erode, become entrained in the plasma, and redeposit over PFMs. Concerns regarding maintaining the T fuel cycle and nuclear facility licensing necessitate the projection, monitoring, and control of T inventory.

To accurately project T accumulation, the companion paper [2] outlines the expansion of predictive Be-HI scaling developed previously [3] to a deposition parameter space that is more ITER relevant. That paper [2] also reports the modeling of Single-Layer (SL) Be–D co-deposits in TMAP-7 [4, 5].

ITER plans to maintain T inventory below the in-vessel administrative limit of 700 g [6]. A strategy to remove T is the baking of PFMs, namely the first wall and divertor at 513 K and 623 K, respectively. Though baking has been shown to remove the majority of HI at 623 K, the continual co-deposit growth may be of concern as repeated plasma and bake cycles will deposit new over-layers on top of previously baked

under-layers. Previous work [7, 8] studying co-deposit thickness and under-layer baking on HI retention showed both issues had a deleterious effect on bake efficiency; thicker layers took longer bake time to remove HI and that an oxide layer formed during the bake may have impeded the removal of HI in an under-layer. We further investigate the bake efficiency on Double-Layer (DL) samples by testing if bake duration influences the induced Be–O layer and associated effects.

2. Experiment

Detailed experimental procedure can be found in [2] and relevant details for this experiment are as follows. W spheres of 5 mm diameter, received multiple Be coatings in the PIS-CES-Be magnetron sputter coater in an Argon (Ar)–Deuterium (D) background plasma at $T_{dep} = 393$ K, $R_{dep} = 3 \times 10^{19}$ m^{-2} s^{-1}, $p = 0.8$ Pa, and $E_{dep} = 40$ eV. Note that Ar facilitates increased Be sputter rate and is minimally retained in the co-deposits ($<0.1\%$) as measured by TDS [2]. Figure 1 outlines the experimental scheme for various SL, DL, and baked DL (bDL) spheres. As described

---

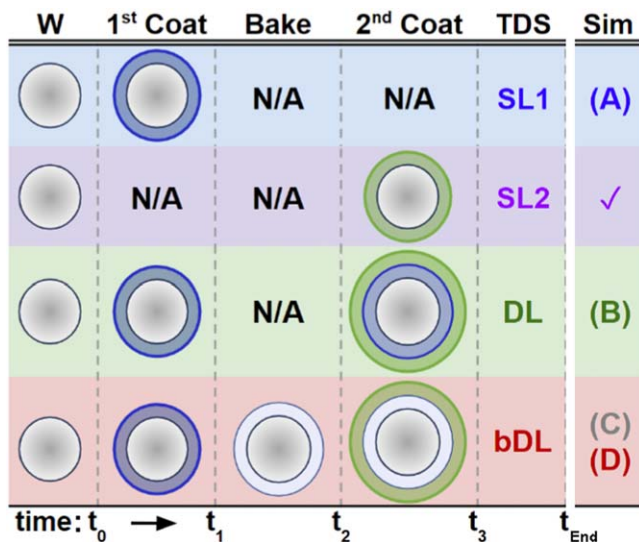[3] Author to whom any correspondence should be addressed.

Figure 1. Multi-layer diagram depicts 1st coat (SL1 in blue), 2nd coat (SL2 in purple), and both coatings (DL in green). Select SL spheres were baked at 623 K to deplete D filled traps prior to 2nd coat (bDL in red). TMAP simulations (A)–(D) are detailed in sections 4 and 5.
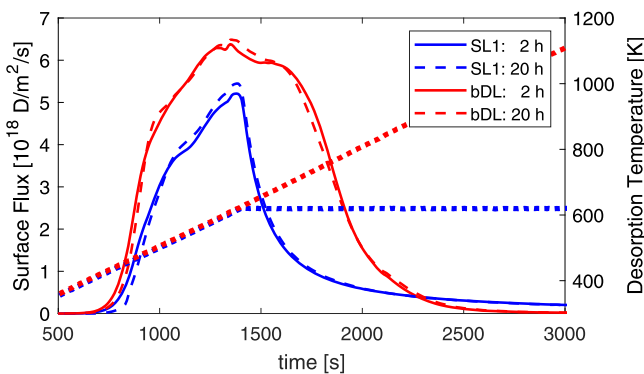

Figure 2. Two samples from a batch of SL1 spheres were baked/desorbed for 2 and 20 h, respectively (blue). After a 2nd coating, the TDS of the bDL spheres (red) are nearly identical in flux. Temperature history (right axis) for bake (blue) and TDS (red) are dotted lines.

in [9], Wavelength Dispersive x-ray microanalysis quantified oxidation caused by baking, relative to the as-deposited state. After final coating, each sphere performed a full TDS run up to 1273 K with ramp rate $0.3\,\mathrm{K\,s^{-1}}$.

3. Results

Samples prepared with a bake phase before the application of the 2nd coat (i.e. bDL in figure 1) were heated at $0.3\,\mathrm{K\,s^{-1}}$ and held at 623 K for either 2 or 20 h. Between over- and under-layers, these baked spheres developed a 2 and 4 nm thick oxide layer, respectively. Figure 2 shows that the D released from each co-deposit during the flattop bake and during the full TDS (after receiving a 2nd coat) were nearly identical for both a 2 and 20 h bake. The bake phase (blue)
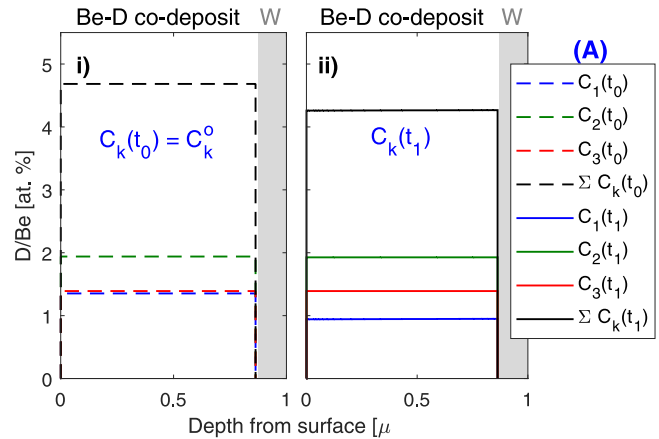

Figure 3. SL1 TMAP simulation (A) assumes the full deposited layer with completely filled traps at t_0 (i). This layer is held at the peak deposition temperature to thermally relax the trapped D up to time t_1 (ii). Traps 1–3 correspond to detrap energies 0.8, 0.9, and 1.0 eV.

shows exponentially diminishing D release during the 623 K hold (blue dotted line on temperature axis).

4. TMAP modeling

This work expands upon the previous work modeling Be–D co-deposits in TMAP [10]. The bulk and transport properties for D in pure Be are taken from table 1 of that work. Only the sample surface exposed to vacuum allows D to escape, as the boundary condition on the inner surface facing W is modeled with zero flux. Using the larger TDS data set with varied deposition parameters obtained in [2], the number of traps and associated detrapping energies were varied during simulations and determined to be 3 traps at 0.8, 0.9, and 1.0 eV. The D released during TDS divided by the co-deposit thickness constrains the total filled D trap concentration after co-deposition (i.e. prior to TDS). The individual trap concentration (C_k^o) and D filled trap concentration (C_k) are unknown. To reduce the number of free parameters, only C_k^o was allowed to vary and C_k was determined by simulation as follows.

Since TMAP was developed with static trap concentrations, we did not simulate a growing co-deposit layer. Instead, the entire layer is defined at time t_0 and all traps are completely filled with D initially. Next, a thermal relaxation simulates the elevated sample temperature during co-deposition that allows D out-gassing and trap depopulation. The D filled trap concentration remaining after this phase is approximated by holding the sample fixed at the peak co-deposition temperature for the total co-deposition time-at-temperature. Following the hold, to allow mobile D to either re-trap or escape the surface, we simulate a relatively short ramp down to room temperature ending at time t_1. Figure 3 details each trap and D fill concentration at t_0 and after thermal relaxation at t_1 for TMAP simulation (A). Shown in figure 4, the TDS phase is simulated with a $0.3\,\mathrm{K\,s^{-1}}$ linear temperature ramp and compared to experiment.
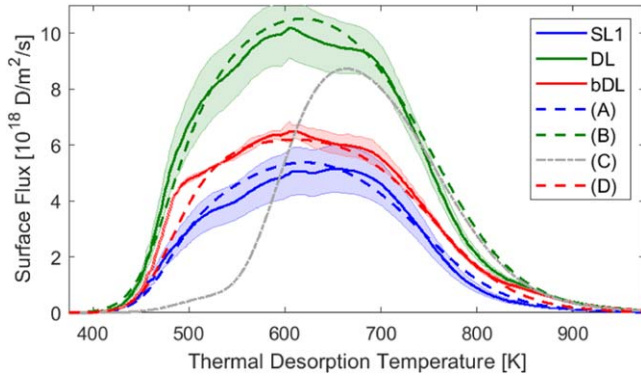
Figure 4. The averaged TDS profiles (solid lines) from two RGAs are shown with a shaded error band. Single-layer spheres (blue) were coated after a bake (red) or without a bake (green). TMAP Simulations (dashed) (B)–(D) are detailed in section 5.

5. Multi-layer bake efficiency

Figure 1 outlines this test on the effect of baking a co-deposit prior to a 2nd coating. The best fit to the SL1 case resulted from the TMAP simulated trap profile (A) detailed in figure 3. Each sphere produced in the same batch produced a desorption flux with a high degree of repeatability as shown in figure 2. SL2 was fit to TDS data with similar trap concentrations to SL1 (not shown here). Thus the trap profile for SL1 was used as the under-layer and the trap profile for SL2 was used as subsequent over-layer modeled in TMAP (i.e. DL and bDL). The high repeatability of TDS data from the same batch of coatings constrains the total trap concentrations for each layer, allowing only the individual sample history to adjust the D fill levels. That is, a self-consistent simulation of the DL and bDL samples must have the same trap concentrations as the SL1 and SL2 for under- and over-layers.

To simulate the DL, the 2nd coat produced an over-layer on top of the 1st coat, where the respective trap concentrations for SL2 and SL1 were previously fit. At time t_2, the under-layer D fill concentration is equal to SL1 at time t_1 (figure 3(ii)) while the over-layer is assumed completely full. Next, trap populations for both layers are allowed to thermally relax as previously described for the SL until t_3 as shown in figure 5(B). The resulting TMAP simulation in figure 4 agrees well with the TDS data.

Similar to the DL, the simulation for the bDL also assumed the SL1 at time t_1 for the under-layer. Prior to adding the over-layer, the bake thermal history from time t_1 to t_2 was simulated causing profile (A) to further depopulate D. Next, the over-layer with SL2 trap concentrations are assumed completely filled and placed on top of the baked under-layer at t_2. Finally, the trap concentrations are allowed to thermally relax until t_3.

Following this procedure for bDL produces TMAP simulation (C) in figure 5. Note that the apparent discontinuity for filled traps at the boundary between layers is due to the different trap concentrations for SL2 and SL1 (i.e. the over- and under-layers). The traps emptied by the bake are partially re-filled during the 2nd coating. This case effectively *pumps* D from the over-layer into the under-layer. The TDS
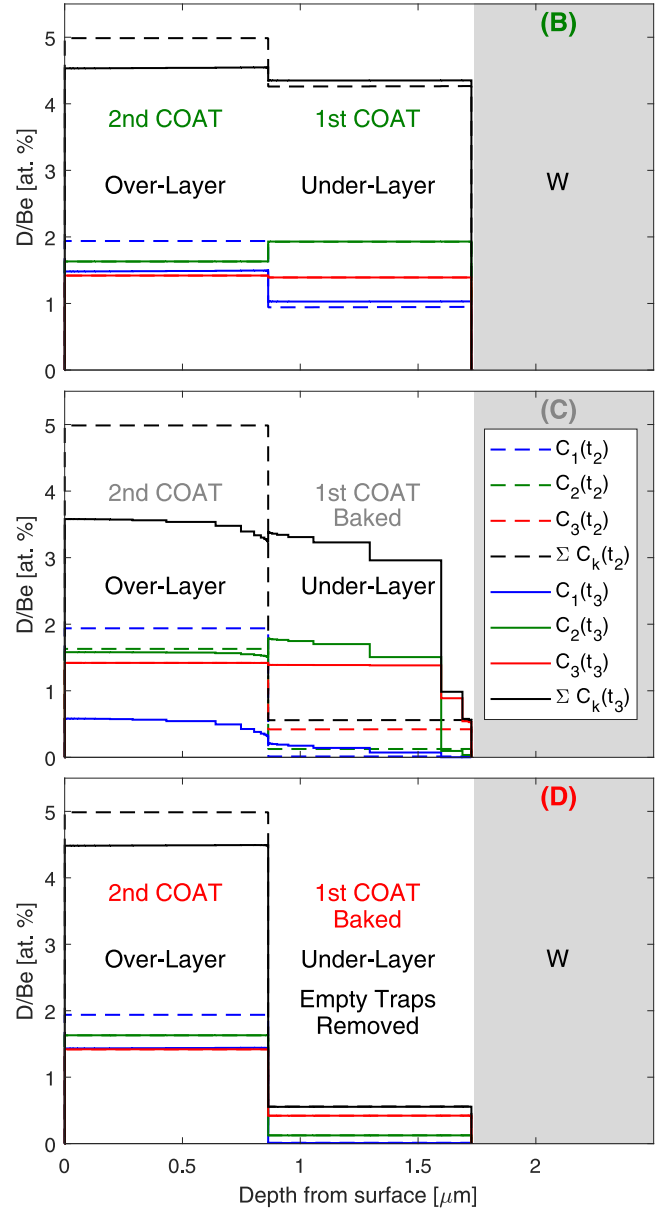

Figure 5. TMAP simulations (B)–(D) depict the (D) filled trap concentrations prior to (t_2) and after final thermal relaxation (t_3). Subsequent simulated thermal desorption for each case are shown in figure 4: (B) satisfies the DL (green dashed line), (C) diverges from bDL (grey dotted–dashed line), and (D) agrees with the bDL (red dashed line) desorption fluxes.

simulation results in the grey dashed D surface flux in figure 4. This does not correspond to the bDL experimental data (solid red). The pumping action degrades bake efficiency by shifting the thermal desorption towards higher temperature.

In a similar experiment with nearly identical conditions, Baldwin *et al* [8] prepared Be–D multi-layer co-deposits. After the baking phase, a ~40 nm thick Be–O layer was measured and it was postulated that the oxide acted as a diffusion barrier between the over- and under-layers. Reported in section 3, the oxide layers produced in this experiment by a 2 and 20 h bake (2 and 4 nm) are too thin to produce a similar effect as seen in [8]. A surface oxidation diffusion

barrier is therefore not able to explain the lack of under-layer pumping of D, as simulation (C) suggests should occur when empty traps are present.

Maintaining the same trap parameters from the SL and DL, the only plausible change in the bDL is the total trap concentrations after the bake. We therefore postulate that baking the Be–D co-deposit may lead to trap annealing. Removing all empty traps prior to the thermal relaxation of the 2nd coating results in case (D). The resulting full TDS (dashed red) in figure 4 is a much closer match to the experimental data (solid red).

6. Conclusion

Modeling of Be-HI DL samples suggests during baking of the SL, both the trapped HI and the empty traps themselves are removed from this under-layer. With the pumping effect in play, each successive bake cycle after each new co-deposition layer would shift the trapped HI to higher desorption temperature and cause the inventory to grow. Furthermore, HI would diffuse both toward the surface as well as deeper into the under-layers of the co-deposit. This work shows there is little pumping effect into the under-layer, resulting in the removal of most of the trapped HI. With respect to a cycle of ITER divertor bakes, subsequent over-layers will behave more similar to a SL than the less-efficient-to-desorb multi-layer system with empty traps. That is, during a fresh Be-T coating, the baked under-layers will not pump T and act as a refillable reservoir.

Acknowledgments

ORCID iDs

M J Simmonds ● https://orcid.org/0000-0003-2238-4386
M J Baldwin ● https://orcid.org/0000-0001-6335-2255
G De Temmerman ● https://orcid.org/0000-0002-4173-0961

References

[1] Roth J *et al* 2009 *J. Nucl. Mater.* **390** 1–9
[2] Baldwin M, Simmonds M, De Temmerman G and Doerner R 2019 *Phys. Scr. PFMC Proc.* (https://doi.org/10.1088/1402-4896/ab41a3)
[3] De Temmerman G, Baldwin M, Doerner R, Nishijima D and Schmid K 2008 *Nucl. Fusion* **48** 075008
[4] Merrill B, Jones J L and Holland D 1986 TMAP/Mod 1: Tritium Migration Analysis Program code description and user's manual *Technical Report* (Idaho Falls, ID: EG and G Idaho Inc)
[5] Longhurst G 2008 TMAP7 user manual *Technical Report* EXT-04-02352 Rev. 2(Idaho Falls, ID: Idaho National Engineering and Environmental Laboratory)
[6] De Temmerman G, Baldwin M, Anthoine D, Heinola K, Jan A, Jepu I, Likonen J, Lungu C, Porosnicu C and Pitts R 2017 *Nucl. Mater. Energy* **12** 267–72
[7] Baldwin M and Doerner R 2015 *J. Nucl. Mater.* **467** 383–91
[8] Baldwin M and Doerner R 2014 *Nucl. Fusion* **54** 083032
[9] Roth J, Doerner R, Baldwin M, Dittmar T, Xu H, Sugiyama K, Reinelt M, Linsmeier C and Oberkofler M 2013 *J. Nucl. Mater.* **438** S1044–7
[10] Baldwin M, Schwarz-Selinger T and Doerner R 2014 *Nucl. Fusion* **54** 073005